International Journal of Electrical and Computer Engineering (IJECE)
Vol. 10, No. 3, June 2020, pp. 2402~2415
ISSN: 2088-8708, DOI: 10.11591/ijece.v10i3.pp2402-2415

Tuning of different controlling techniques for magnetic suspending system using an improved bat algorithm

Nizar Hadi Abbas
Department of Electrical Engineering, College of Engineering, University of Baghdad, Iraq

Article Info

Article history:

Received Sep 28, 2019
Revised Nov 5, 2019
Accepted Nov 25, 2019

Keywords:

Benchmark test functions
Improved bat algorithm
Magnetic suspending system
PD, PDF and PDFF controllers
Standard bat algorithm

ABSTRACT

In this paper, design of proportional- derivative (PD) controller, pseudo-derivative-feedback (PDF) controller and PDF with feedforward (PDFF) controller for magnetic suspending system have been presented. Tuning of the above controllers is achieved based on Bat algorithm (BA). BA is a recent bio-inspired optimization method for solving global optimization problems, which mimic the behavior of micro-Bats. The weak point of the standard BA is the exploration ability due to directional echolocation and the difficulty in escaping from local optimum. The new improved BA enhances the convergence rate while obtaining optimal solution by introducing three adaptations namely modified frequency factor, adding inertia weight and modified local search. The feasibility of the proposed algorithm is examined by applied to several benchmark problems that are adopted from literature. The results of IBA are compared with the results collected from standard BA and the well-known particle swarm optimization (PSO) algorithm. The simulation results show that the IBA has a higher accuracy and searching speed than the approaches considered. Finally, the tuning of the three controlling schemes using the proposed algorithm, standard BA and PSO algorithms reveals that IBA has a higher performance compared with the other optimization algorithms.

Corresponding Author:

Nizar Hadi Abbas,
Department of Electrical Engineering,
College of Engineering, University of Baghdad,
Aljadriya district, Baghdad, Iraq.
Email: dr.nizar.hadi@coeng.uobaghdad.edu.iq, drnizaralmsaodi@gmail.com

1. INTRODUCTION

The use of magnetic suspending (levitation) technology eliminates the physical contacts between moving and stationary parts through suspending objects in air without any support. Magnetic levitation (maglev) is an unstable control system with fast dynamics behavior. Magnetic suspending system (MSS) gained a great interest by the researchers because of its importance in engineering applications and industries. Therefore, researchers studied different controlling schemes in order to stabilize the system and enhance their performances such as classical analogue controllers, classical discrete controllers and modern controllers.

Present an optimized PID controller to control the metal ball position of the MSS based on grey wolf optimizer (GWO) algorithm [1]. Introduced a classical PID controller for controlling the maglev system using teaching learning based optimization (TLBO) algorithm, which is a well-known meta-heuristic technique to find out the optimum values of PID parameters [2]. The authors claim that the suggested controlling techniques provide better time domain and frequency-domain specifications. Designed a PID controller for Maglev system basing on the particle swarm optimization (PSO) algorithm with four inertia weights, namely, Fixed Inertia Weight (FIW), Linear Descend Inertia Weight (LIW), Linear Differential Descend Inertia Weight (LDW), and mixed inertia weight (FIW–LIW-LDW). They found that the controlling performances of PSO-PID with mixed inertia weights are better than that with single inertia weights [3].

Used genetic algorithm (GA) in tuning the parameters of PID controller designed for MSS system. They compared their results with the Ziegler and Nichols tuning method and found that their method gives better performance [4].

Investigate the modelling and variable structure controller design of an MSS with system parameters' uncertainty. The author used variable structure control scheme based on Lyapunov function method to attenuate the chattering effect and therefore, pushing the position of the ball to different desired places. The researcher obtained acceptable steady-state error value for the ball position [5]. Developed of a control system for a single degree of freedom MSS to achieve a stable suspending of a steel ball at specified distance using IMC-based PID controller. The suggested controller gives better closed-loop performance after using a setpoint filter [6].

Used the least square estimation in modeling Maglev system by considering the change in the current as an input and the change in a ball position as an output and state feedback controller and LQR controller to enhance the system performance [7]. Discussed Maglev model for magnetic levitation system theoretically, and took two types of compensators (proportional-Derivative and Phase-lead). They concluded that the unstable Maglev system can be stabilized by using suitable controlling parameters of the compensators [8].

Suggest an efficient fuzzy logic controller (FLC) using triangular membership function, and the collected results are compared with the classical PD controller. The simulation results claimed that the FLC controller performed satisfactorily with two different input signals [9]. Present an FLC controller that applied to a simple MSS, also a linearized model is formulated to design a discrete classical PID controller. Furthermore, a decomposed fuzzy PID controller is utilized to compare the performance of the three suggested controlling schemes. The simulation results claimed that fuzzy PID controller based on decomposed inference method provide high-speed control performance [10]. Another work on stabilizing Maglev system was presented by A. H. Fares et al. [11], using a PD fuzzy controller to keep the balance between the magnetic force and the ball's weight is the main function of PD fuzzy controller. The authors concluded that the stability of the magnetic levitation was improved using fuzzy PD controller.

In this research work, a mathematical model for MSS is developed; three different controlling techniques for the MSS are designed based on BA and PSO algorithms. An improved BA (IBA) is proposed to enhance the performance of the maglev system under uncertainty. The proposed algorithm and the standard algorithms are examined to test their capability by solving a set of benchmark problems, and the obtained results are analyzed based on various statistic parameters. Therefore, the proposed algorithm with the other standard algorithms are utilized to find out the tuning parameters of the three controlling methods to achieve the paper target which is improving the system performance and increases the system robustness's.

The rest of the paper is arranged as follows: The model of magnetic suspension system is presented in Section 2, talks about MSS. In Section 3, the controlling techniques (PD, PDFF and PDF) and standard Bat algorithm are introduced. The proposed improved Bat optimization algorithm is explained in Section 4. Tunings of the controlling schemes and Fitness function formulation for tuning the controllers are presented in Section 5. In Section 6, the proposed algorithm evaluation, the system performance, and a detailed discussion for the results are illustrated in Section 6. Finally, a brief conclusion is given in the last Section.

2. MAGNETIC SUSPENDING SYSTEM MODEL

Magnetic suspending system, constructed mainly from four major components: the ferromagnetic steel sphere suspended in a voltage-controlled magnetic field, infrared ball position sensors, controller and actuator [12]. The schematic diagram of MSS is shown in Figure 1 [13]. The magnetic suspending technology disregarded the friction problem between moving and stationary parts; therefore, the main goals of MS system are used to retain the metal ball in a specified vertical level in practical engineering applications such as high-speed magnetic levitation trains, wind tunnel levitation etc. MSS is inherently nonlinear and unstable system described by nonlinear D.E. The MSS dynamic equations [14, 15].

$$\boldsymbol{v} = \frac{\boldsymbol{dx}}{\boldsymbol{dt}} \tag{1}$$

$$e = V_R + V_L = R\, i + \frac{d(L(x)i)}{dt} \tag{2}$$

$$m\, \dot{v} = m\, g - c\, \left(\frac{i}{x}\right)^2 \tag{3}$$

where, v denotes the ball's velocity, x is the ball's position, e is the applied voltage, R is resistance of the coil, $L(x)$ is the inductance coil, i the coil's current, g is the gravitational constant, m is ball's mass, c is the constant of the magnetic force.

The inductance $L(x)$ is a non-linear function of the ball's position. Several approximation methods can be used for finding the inductance for the system. The important approximation is done based on the inductance should be inversely proportional to the position of the ball as follows:

$$L(x) = L_1 + L_0\, x_0 / x \tag{4}$$

where, x_0 is arbitrary reference for the inductance, L_1 is the coil's inductance in the absence of a L_0 is the additional coil's inductance resultant from the ball's presents.

In order to formulate the linearized state space representation, substitute (4) in (2) with taking the state assumptions as; $x = x_1$, $v = x_2$, $i = x_3$, & $u = e$ and linearizing the model under the equilibrium point, $(x_{10}$, x_{20} , x_{30}) = $(x_0$, 0 , $i_0)$ with reference input $u_0 = R\, x_{30}$. Finally, the linearized MSS state model is as follows:

$$A = \begin{bmatrix} 0 & 1 & 0 \\ K_1 & 0 & K_2 \\ 0 & K_3 & K_4 \end{bmatrix},\ B = \begin{bmatrix} 0 \\ 0 \\ 1/L_C \end{bmatrix} \quad and \quad C = [1 \quad 0 \quad 0] \tag{5}$$

where:

$$K_1 = \frac{2KI^2}{my_o^3},\ K_2 = \frac{-2KI}{my_o^2},\ K_3 = \frac{2KI}{L_C y_o^2} \ \&\ K_4 = \frac{-R}{L_C} \tag{6}$$

After knowing the state space model, the system transfer function will be:

$$G_P(S) = \frac{K_2/L_C}{S^3 - K_4 S^2 - (K_1 + K_2 K_3)S + K_1 K_4} \tag{7}$$

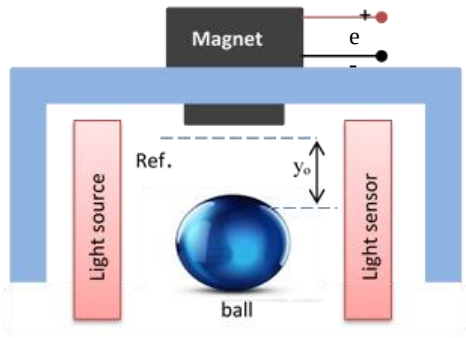

Figure 1. Schematic diagram of MS system

After substitute the MSS model parameters' values from Table 1, the transfer function becomes,

$$G_P(S) = \frac{-1420}{S^3 + 283.5\, S^2 + 392.4\, S - 551900} \tag{8}$$

Table 1. Parameter setting of magnetic MS system

Parameter	Definition	Value	Unit
m	Mass of ball	0.01058	Kg
L_C	Coil inductance	0.1097	H
R	Coil resistance	31.1	Ohm
I	Current	0.125	A
y_o	Ball position	0.01	m
K	Constant	0.00065906	Nm^2/A^2
K_S	Gain of light sensor	-156	V/m

3. THEORETICAL BASICS

3.1. Controlling techniques

In this section, control schemes like proportional-derivative (PD) controller, pseudo-derivative-feedback (PDF) controller, and pseudo-derivative-feedback with feedforward term (PDFF) controller are proposed. Overall closed-loop representations of the MS system with series control schemes are illustrated in Figure 2. These control schemes are explained in details in the following subsections.

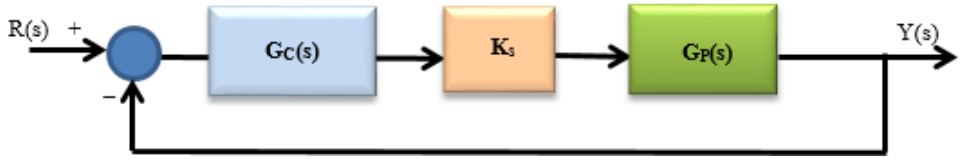

Figure 2. Overall closed–loop representation of the MSS with control scheme

3.1.1. PD controller

The actuating signal for PD control action consists of proportional error signal added with derivative error signal. Therefore, the actuating signal for PD control action is given by:

$$e_a(t) = K_P\, e(t) + K_D\, \frac{d\, e(t)}{dt} \tag{9}$$

where K_P and K_D are the proportional and derivative constants, respectively.

The Laplace transform of the actuating signal is as follows:

$$E_a(S) = K_P\, E(S) + S\, K_D\, E(S) \tag{10}$$

and the transfer function of PD series controller is:

$$G_c(S) = K_P + S\, K_D \tag{11}$$

The optimal design of PD controller will affect the performance of an MSS through reducing the settling time, and peak overshoot as well as improves the gain and phase margins [10].

3.1.2. PDF controller

The pseudo-derivative-feedback (PDF) controller is shown in Figure 3.

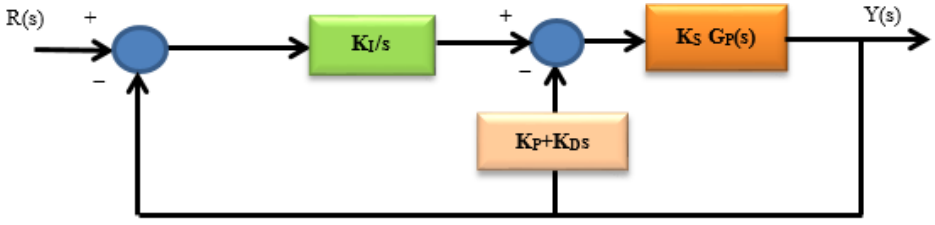

Figure 3. Overall closed–loop representation of the MSS with PDF (pseudo derivative-feedback) controller

where K_P, K_D and K_I are respectively the proportional, the derivative and the integral parameters.

The reason behind moving the proportional and derivative actions from the feedforward path to a feedback path is that it causes a sudden change in the actuating error signal, where the physical limitations of the differentiating device cause the calculation of the derivative to be incorrect, thus, accordingly, the actual system's performance will be smaller than the ideal performance set by the MSS model [16]. The integral action is kept in the feedforward path to avoid the static error.

The actuating signal for PDF controlling scheme is as follows:

$$e_a(t) = K_I \int e(t)\, dt - K_P\, y(t) - K_D \frac{d\, y(t)}{dt} \quad (12)$$

and the PDF controller transfer function can be determined implicitly with the overall system closed loop T.F through using Mason's reduction formula.

3.1.3. PDFF controller

The pseudo-derivative-feedback with feedforward term (PDFF) controller is illustrated in Figure 4. A PDFF controller has the integral action in the forward path to eliminate the steady-state error, while the proportional and derivative actions which located in the feedback path are used to enhance the response (gain margin, phase margin, and disturbance rejection…etc.). The feedforward gain K_{FF} is utilized to regulate the input variations. Therefore, the PDFF controller will overcome the slow response specifications and maintaining the stability during the optimization process [17].

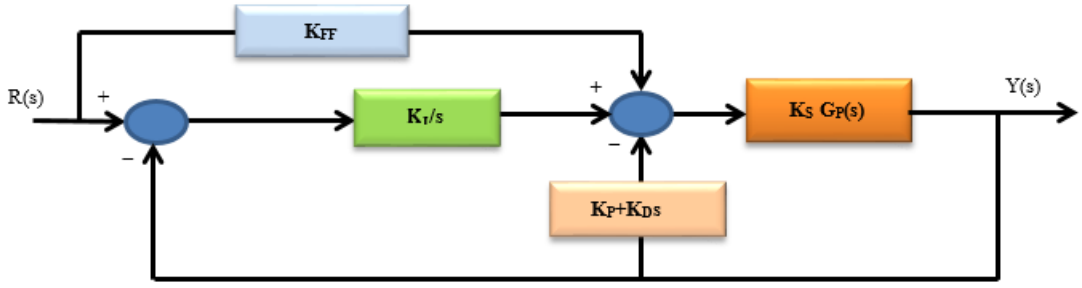

Figure 4. Overall closed –loop representation of the MSS with PDFF (pseudo-derivative-feedback with feedforward term) controller

The actuating signal for PDFF control action is as follows:

$$e_a(t) = K_I \int e(t)\, dt + K_{FF}\, r(t) - K_P\, y(t) - K_D \frac{d\, y(t)}{dt} \quad (13)$$

and the PDFF controller transfer function can be obtained implicitly with the overall system closed loop T.F by using Mason's gain rule.

3.2. Standard bat algorithm

The standard Bat algorithm (SBA) is a bio-inspired based metaheuristic optimization technique. It was invented by X.-S. Yang [18] in 2010 for solving constrained continuous optimization problems. Bats are the only mammals with wings, and they also have advanced capability of echolocation. Bats use a type of sonar, called echolocation process, to detect prey, avoid obstacles and locate their roosting crevices in the dark [19]. These Bats use time delay measurements between transmitted sound pulses and the reflected pulses for navigation through dark environment and hunt. The time delay is utilized to measure how far away a prey and food are. They typically emit short and very loud sound with duration 10 to 20 times per second with inbound frequencies ranging from 25 to 125 KHz [20]. SBA is implemented by using the following three generalized rules [21]:

- The Bats use the echolocation process to measure the distance and to distinguish between prey and food.
- The Bats fly randomly with velocity v_i at position x_i and producing pulses with a fixed frequency f_i and loudness A_i.
- The frequencies f_i and rate r_i of each pulse is adjusted automatically depending on the proximity of the target.

According to specific objective function, one value for position, velocity, frequency and loudness will be the best. After that these parameters will be updated at each iteration, and the best values are determined. The SBA procedure with a mathematical formula can be summarized as in the Algorithm 1 shown below:

Algorithm 1. Standard bat algorithm
Before starting,
Define:

- The population size (number of bats=25),
- The number of generations (number of iterations=100),
- Loudness (A=0.25),
- Pulse rate (r=0.5),
- Frequency range (f_{min}=0, f_{max}=2)
- Number of dimensions (number of variables "d")
  = 2 for the PD controller K_D & K_P
  = 3 for PDF controller K_I, K_D & K_P
  = 4 for the PDFF controller K_I, K_{FF}, K_D & K_P
- Generate the initial population of frequency, velocity and position:

$frequency$: $f = \begin{bmatrix} 0 & \cdots & 0 \\ \vdots & 0 & \vdots \\ 0 & \cdots & 0 \end{bmatrix}_{n*d}$ and $velocity$: $v = \begin{bmatrix} 0 & \cdots & 0 \\ \vdots & 0 & \vdots \\ 0 & \cdots & 0 \end{bmatrix}_{n*d}$

Position, *x* takes random values between min and max for each variable;

for the PD controller $x = \begin{bmatrix} K_{D\,min} & K_{P\,min} \\ \vdots & \vdots \\ K_{D\,max} & K_{P\,max} \end{bmatrix}$

for the PDF controller $x = \begin{bmatrix} K_{I\,min} & K_{D\,min} & K_{P\,min} \\ \vdots & \vdots & \vdots \\ K_{I\,max} & K_{D\,max} & K_{Pmax} \end{bmatrix}$

for the PDFF controller $x = \begin{bmatrix} K_{I\,min} & K_{FF\,min} & K_{D\,min} & K_{P\,min} \\ \vdots & \vdots & \vdots & \vdots \\ K_{I\,max} & K_{FF\,max} & K_{D\,max} & K_{P\,max} \end{bmatrix}$

Step1: The initialization
Evaluate the objective function (fitness) for each bat, then find G_{best} (the min. value).
Step 2: Movement of virtual bats
Start bat algorithm with A=0.25, r=0.5 [18].

- Start iteration counter
- Update the bat population for each bat according to these equations,

$$\boldsymbol{f_i = f_{min} + (f_{max} - f_{min})\beta}$$
$$\boldsymbol{v_{i.m}^{t+1} = v_{i.m}^{t} + (X_{i.m}^{t} - X_{Gbest.m})f_i}$$
$$\boldsymbol{X_{i.m}^{t+1} = X_{i.m}^{t} + v_{i.m}^{t+1}\Delta t}$$

Where: *i=1, 2, -----n* and *m=1, 2, -----, d.*
The SBA variables and parameters are defined in Table 2.

- for β>r

$$\boldsymbol{X_{new} = X_{Gbest} + \epsilon A^t}$$

Where: $\boldsymbol{\epsilon} \in$ [-1,1] which is a random number.
and $A^t=<A_i^t>$ which is the average loudness of all the bats at iteration *t*.

- Diagnose X_{new} if it is still in range using X_{min} and X_{max} for each variable
- Evaluate new solutions (F_{new}) by taking the fitness for the updating values then comparing with the old ones (F_{min}).
  If $F_{new}<F_{min}$ Then F_{new} will be the best
  Display the result for the first iteration

Step 3: Loudness and Pulse Emission

- Starting from iteration number 2
- update the bat population as it was explained in step 2 (in other words repeat step 2 with different values of A (loudness) and r (pulse rate)) according to the following equations, α=0.9 ; γ=0.9 ;

$$A_i^{t+1} = \alpha A_i^t$$
$$r_i^{t+1} = r_i^0[1 - \exp(-\gamma * t)]$$

The parameters are defined in Table 2.

- Repeat the iteration.
  Display the final results.

End of standard Bat algorithm

Table 2. The description of standard bat algorithm variables and parameters

Variables and Parameters	Description
n	Number of bats in the swarm
d	Search space dimension
t	Current iteration
f	Is the frequency in a range [f_{min}, f_{max}]
β∈[0,1]	Is a random vector drawn from a uniform distribution
$\boldsymbol{v_{i.m}^t}$	Current velocity of bat *i* at iteration *t*
$\boldsymbol{v_{i.m}^{t+1}}$	Updated velocity of bat *i*
$\boldsymbol{X_{i.m}^t}$	Current position of bat *i* at iteration *t*
$\boldsymbol{X_{Gbest.m}}$	Current global best location (solution) which is located after comparing all the solutions among all the *n* bats for each *m*.
$\boldsymbol{X_{i.m}^{t+1}}$	Updated position of bat *i*
$\boldsymbol{\Delta t}$	Time step which is taken to be unity
$\boldsymbol{A_i^t}$	The loudness of a bat *i* at iteration *t*
$\boldsymbol{A_i^{t+1}}$	Updated loudness of bat *i* [initial loudness $A_i^0 \in [1,2]$]
α	Constant drawn from 0<α<1
$\boldsymbol{r_i^{t+1}}$	Updated pulse emission rate of bat *i*
$\boldsymbol{r_i^0}$	Initial pulse emission rate ∈[0,1]
γ	Constant drawn from γ>0 {for simplicity, usually can use γ=α=0.9}
For any 0<α<1 and γ>0, apply $A_i^t \to 0. r_i^t \to r_i^0, as\ t \to \infty$	

4. IMPROVED BAT ALGORITHM

This paper proposes three modifications to enhance the SBA in order to finding global optimum solutions as explained in the following subsections.

4.1. Modified frequency factor

This modification approach will update the frequency value during the optimization process.

$$f_i = \left[\frac{f_{max}+f_{min}}{2} + \frac{f_{max}-f_{min}}{2} log_{10}\left(100\left(\frac{t_{max}-t}{t_{max}}\right)\right)\right]\beta \quad (14)$$

The frequency adaptation equation is formulated by several running of standard Bat algorithm.

4.2. Adding inertia weight factors

The inertia weight factor control exploration and exploitation of a particle swarm optimization (PSO) algorithm, is more like local searching algorithm. On the other hand, when inertia weight is large PSO algorithm is more like global search method [22]. In order to provide balancing between local and global exploration and better convergence rate in standard Bat algorithm, the paper proposes the inertia weigh factors as in the PSO algorithm [23]. In this research, the following four equations have been derived to satisfy a better optimization process

$$V_{i,m}^{t+1} = W_1^t V_{i,m}^t + \left(X_{i.m}^t - X_{Gbest,m}\right) f_i \quad (15)$$

$$X_{i,m}^{t+1} = W_2^t X_{i,m}^t + V_i^{t+1}\Delta t \quad (16)$$

where:

$$W_1^t = (W_{max} - W_{min})\ sin\left(\frac{\pi}{2}\left(\frac{t_{max}-t}{t_{max}}\right)\right)^2 + W_{min} \quad (17)$$

$$W_2^t = (W_{min} - W_{max})\ exp\left(-5\left(\frac{t}{t_{max}}\right)^2\right) + W_{max} \quad (18)$$

W_{min} =0.4 and W_{max} = 0.9

4.3. Modified local search

Here with defining the dynamic S^T scale factor parameter (a factor that limits the step sizes of random walks for local search), an improvement is proposed for this algorithm. Proper tuning of this parameter reduces the number of iterations and therefore, the computation's time is reduced accordingly. Dynamic scale factor *S* parameter may be formulated as:

$$S^T = (S_{max} - S_{min}) exp\left[\left(\frac{ln\left(\frac{S_{min}}{S_{max}}\right)}{S_{max}}\right)\left(\frac{t_{max}-t}{t_{max}}\right)\right] + S_{min} \quad (19)$$

Instead of using

$$X_{new} = X_{Gbest} + \epsilon A^t$$

For modified local search, the following equation can be used

$$X_{new} = X_{Gbest} + \epsilon S^t \quad (20)$$

where,
t: current iteration
t_{max}: maximum number of iterations
S_{max} and S_{min} should be taken such as 1 and 0.001 respectively [24].

The IBA procedure with a mathematical formula can be summarized as in the Algorithm 2 illustrated below.

Algorithm 2: Improved Bat algorithm
Before starting,
Do the same as in Standard Bat algorithm
Step 1: Initialization
Calculate the fitness for each bat then find the min one (the best one) according to objective function.
Step 2: Movement of virtual bats
Start Bat algorithm with A= 0.25, r= 0.5 [18].

- Start iteration counter
- Define W_{min}=0.4; W_{max}=0.9; S_{max}=1; S_{min}=0.001;
- Update the frequency, inertia weight ($\boldsymbol{W_1^t}$), velocity, inertia weight ($\boldsymbol{W_2^t}$), and position for each bat according to equations (14), (15), (16), (17), and (18).
- for β> r
  Use Eqs. (19) and (20) to calculate X_{new}
- Diagnose X_{new} if it is still in range using X_{min} and X_{max} for each variable
- Evaluate new solutions (F_{new}) by taking the fitness for the updating values then comparing with the old ones (F_{min}).
  If F_{new} <F_{min} Then F_{new} will be the best
- Display the result for the first iteration.

Step 3: Loudness and Pulse Emission

- Starting from iteration number 2 and ending with iteration *tmax-1* to avoid the division by zero.
- Update the frequency, W_1^t, velocity, W_2^t, and position as in step 2 (in other words repeat step 2 with different values of A (loudness) and r (pulse rate) according to the following equations α=0.9 ; γ=0.9 ;
  $$A_i^{t+1} = \alpha A_i^t$$
  $$r_i^{t+1} = r_i^0[1 - \exp(-\gamma * t)]$$
- Repeat the iteration.
- Display the final results.

End of the improved Bat algorithm

5. TUNING OF CONTROLLING TECHNIQUES

This paper utilized three controlling techniques to control the behavior of magnetic suspending system as explained in the following subsections.

5.1. PD controller tuning

The closed-loop transfer function of the MSS and PD controller is determined as follows:

$$G_{closed-loop\ TF} = \frac{221520\ (K_P + K_D\ S)}{S^3 + 283{\cdot}5\ S^2 + (392{\cdot}4 + 221520\ K_D)S + (221520\ K_P - 551900)} \quad (21)$$

The Routh–Hurwitz criterion is used to find the range of K_P and K_D for stable system.

Condition 1 $K_P > 2.5$ (22)

Condition 2 $\frac{K_P}{K_D} < 283.5$ (23)

The range for K_P and K_D parameters are assumed (by a trial-and-error process) in order to be used in the initialization step in both Algorithms 1 and 2 as follows:
$3 \leq K_P \leq 22$ and $0.075 \leq K_D \leq 0.6$.

5.2. PDF controller tuning

The closed loop transfer function of the MSS and PDF controller is determined as follows:

$$G_{closed-loop\ TF} = \frac{221520\ K_I}{S^4 + 283{\cdot}5\ S^3 + (392{\cdot}4 + 221520\ K_D)\ S^2 + (221520\ K_P - 551900)\ S + 221520\ K_I} \quad (24)$$

In order to find the range for PDF controller's parameters for stable system, the Routh–Hurwitz criterion is utilized.

Condition 1. $K_I > 0$ (25)

Condition 2. $2339.13 + 221520\ K_D - 781.37\ K_P > 0$ (26)

Condition 3. $\frac{-1.3*10^{09} + 9.5*10^{08} K_P - 1{\cdot}2*10^{11} K_D - 6.3*10^{07}\ K_I + 4{\cdot}9*10^{10}\ K_P K_D - 1.7*10^{08}\ K_P{}^2}{2339{\cdot}13 + 221520\ K_D - 781{\cdot}37\ K_P}$ (27)

The range for K_P, K_D and K_I parameters are assumed (by a trial and error process) in order to be used in the initialization step in both Algorithms 1 and 2 as follows:
$\leq K_P \leq 200$, $0.1 \leq K_D \leq 200$ and $0.1 \leq K_I \leq 200$.

5.3. PDFF controller tuning

The closed-loop transfer function of the MSS and PDFF controller is determined as follows:

$$G_{closed\ loop\ TF} = \frac{221520\ (S\ K_{FF} + K_I)}{S^4 + 283{\cdot}5\ S^3 + (392{\cdot}4 + 221520\ K_D)\ S^2 + (221520\ K_P - 551900)\ S + 221520\ K_I} \quad (28)$$

The conditions for stable system are the same of PDF controller's conditions that are determined in Section 5.2. The range for K_P, K_D, K_I and K_{FF} parameters are assumed (by a trial and error process) in order to be used in the initialization step in both Algorithms 1 and 2 as follows:
$0.1 \leq K_P \leq 200$, $0.01 \leq K_D \leq 200$, $0.1 \leq K_I \leq 200$ and $0 \leq K_{FF} \leq 10$.

5.4. Objective function

The objective function is formulated to improve the transient response and guarantee stability of an MS system. In this paper, the objective function is formed by different performance specifications to find out the semi-optimal controller's parameters values using both standard and improved Bat algorithms as described below.

$$\text{Minimize} \quad J = w_1\ t_r + w_2\ t_s + w_3\ (P \cdot O + E_{ss}) \quad (29)$$

where, $\sum_{i=1}^{3} w_i = 1$ which are the weighting factors, t_r is the rising time, t_s is the settling time with 5% error band, $P \cdot O$ is the peak overshoot and E_{ss} is the steady-state error. Let $w_1 = w_2 = w_3 = \frac{1}{3}$. Figure 5 illustrates the overall system blocks which are the magnetic suspending system, the controlling techniques, both optimization algorithms and the objective function with its parameters.

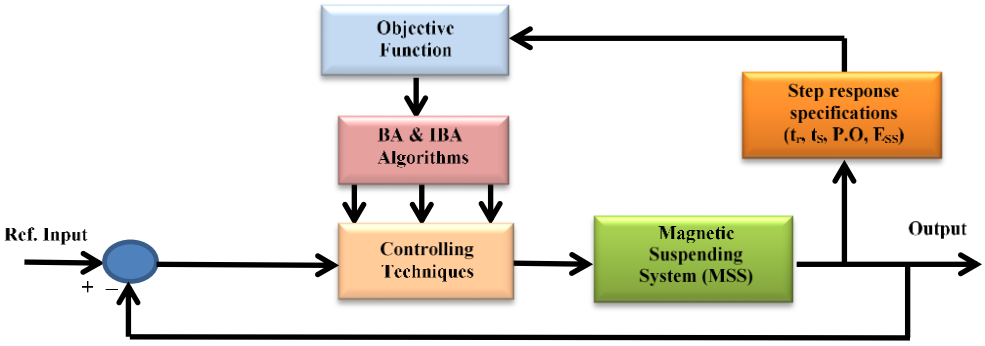

Figure 5. System block diagram

6. SIMULATION RESULTS AND DISCUSSIONS

The simulation results are obtained based on MATLAB R2014a programming language and executing on the system with 2.40GHz CPU and 6.0 G RAM memory. The following sections explain the verification of proposed algorithm quality through utilizing ten benchmark test functions and thereafter, the simulation results are also obtained and discussed.

6.1. Benchmark test functions

To evaluate the performance of the proposed improved Bat algorithm, a set of ten benchmark test functions are used. The standard benchmark set to include unimodal, multimodal, high dimensional and low dimensional optimization functions. A function is multimodal if it has two or more local optima. The algorithm must be able to avoid the regions around the local minimum in order to converge to the global minima. The most complex case appears when the local optima are randomly distributed in the search space. The dimensionality of the search space is another important factor in the complexity of the problem. In general, the complexity increases with the dimensionality. Table 3 shows ten of the well-selected benchmark functions for unconstrained global optimization problem [25].

Table 3. Benchmark test functions

Func. No.	Func. Name	Function Specification D	S	Function Definition	X^*	$f(X^*)$
f1	Ackley	10, 20, 30	[-35, 35]	$f_1(X) = -20e^{-0.2\sqrt{\frac{1}{D}\sum_{i=1}^{D} x_i^2}} - e^{\frac{1}{D}\sum_{i=1}^{D}\cos(2\pi X_i)} + 20 + e$	(0,..,0)	0
f2	Alpine	10, 20, 30	[-10, 10]	$f_2(X) = \sum_{i=1}^{D} \lvert X_i sin(X_i) + 0.1X_i \rvert$	(0,...,0)	0
f3	Brown	10, 20, 30	[-1, 4]	$f_3(X) = \sum_{i=1}^{D-1} (X_i^2)^{(X_{i+1}^2+1)} + (X_{i+1}^2)^{(X_i^2+1)}$	(0, ….,0)	0
f4	Csendes	10, 20, 30	[-1, 1]	$f_4(X) = \sum_{i=1}^{D} X_i^6 \left(2 + sin\frac{1}{X_i}\right)$	(0,..., 0)	0
f5	Paviani	10	[2, 10]	$f_5(X) = \sum_{i=1}^{10} \left[(ln(X_i - 2))^2 + (ln(10 - X_i))^2\right] - \left(\prod_{i=1}^{10} X_i\right)^{0.2}$	(9.35, …, 9.35)	-45.778
f6	Pathological	10, 20, 30	[-100, 100]	$f_6(X) = \sum_{i=1}^{D-1} \left(0.5 + \frac{sin^2\sqrt{100X_i^2 + X_{i+1}^2} - 0.5}{1 + 0.001(X_i^2 - 2X_iX_{i+1} + X_{i+1}^2)^2}\right)$	(0, …, 0)	0
f7	Quintic	10, 20, 30	[10, 10]	$f_7(X) = \sum_{i=1}^{D} \lvert X_i^5 - 3X_i^4 + 4X_i^3 + 2X_i^2 - 10X_i - 4 \rvert$	(-1 or 2)	0
f8	Schaffer	10, 20, 30	[-100, 100]	$f_8(X) = \sum_{i=1}^{D} 0.5 + \frac{sin^2\sqrt{X_i^2 + X_{i+1}^2} - 0.5}{\left[1 + 0.001(X_i^2 + X_{i+1}^2)\right]^2}$	(0, …, 0)	0
f9	Stretched V Sine Wave	10, 20, 30	[-10, 10]	$f_9(X) = \sum_{i=1}^{D-1} (X_{i+1}^2 + X_i^2)^{0.25} \left[sin^2\left\{50(X_{i+1}^2 + X_i^2)^{0.1}\right\} + 0.1\right]$	(0, …, 0)	0
f10	Xin-She Yang Fourth Func.	10, 20, 30	[-10, 10]	$f_{10}(X) = \left[\sum_{i=1}^{D} sin^2(X_i) - e^{-\sum_{i=1}^{D} X_i^2}\right] * e^{-\sum_{i=1}^{D} sin^2\sqrt{\lvert X_i \rvert}}$	(0, …, 0)	-1

Where,
D: Benchmark function dimension.
S: Search space
$f(X^*)$: The optimal objective value that corresponds to the optimal solution X^*.

6.1.1. Simulation parameters settings

In this research, the simulation results are collected with a fixed tolerance $\epsilon \leq 10^{-5}$, and run each algorithm 100 times in order to obtain a meaningful statistical analysis. The parameters that be used in Bat and improved Bat algorithms are as in Algorithm 1 and Algorithm 2. The parameters of PSO algorithm are c_1=c_2 = 1.494 and $w = 0.729$.

6.1.2. Simulation results

The performance of the proposed IBA based on test functions is shown in Table 4. Table 4 illustrates the best, worst and average values obtained by each swarm intelligence based optimization algorithms for different benchmark functions, dimensions and search space. The results of 10 unimodal and multimodal benchmark functions are given in Table 4. According to simulation results, the proposed algorithm improves the original BA's global search capability and provided optimum results, especially for the complex functions f_3 and f_6. Regarding the accuracy and convergence speed of the proposed algorithm is provides a superior and efficient solution compared with other metaheuristics algorithms.

Table 4. Performance comparison between PSO, BA and proposed IBA based on selected benchmark functions

Func No.	D	Iteration	PSO			BA			IBA		
			Optimal	Worst	Average	Optimal	Worst	Average	Optimal	Worst	Average
f1	10	1000	0.0872	3.3346	0.9671	$1.4462*10^{-4}$	$5.7434*10^{-2}$	$3.9621*10^{-2}$	$1.5423*10^{-10}$	$6.5423*10^{-10}$	$3.5219*10^{-10}$
	20	1500	0.1032	5.4463	0.7673	$1.7765*10^{-3}$	$2.0353*10^{-3}$	$2.7176*10^{-3}$	$1.0724*10^{-7}$	$1.7333*10^{-6}$	$1.8174*10^{-5}$
	30	2000	0.2179	6.0063	1.7106	$2.2179*10^{-5}$	$2.9363*10^{-4}$	$3.0064*10^{-3}$	$1.8177*10^{-5}$	$1.9345*10^{-4}$	$1.9980*10^{-3}$
f2	10	1000	55.3114	100.7803	70.6621	0.3462	2.7813	1.7631	$2.0962*10^{-8}$	$11.7452*10^{-6}$	$6.2210*10^{-6}$
	20	1500	89.3936	113.4432	94.9967	0.9564	5.4210	2.9063	$10.8051*10^{-6}$	$42.5376*10^{-4}$	$20.8895*10^{-4}$
	30	2000	103.7602	165.4053	108.9842	1.4712	12.0692	6.0342	$17.7906*10^{-4}$	$45.8044*10^{-3}$	$27.9907*10^{-3}$
f3	10	1000	33.9986	$4.7894*10^{6}$	$8.1348*10^{4}$	5.3289	$2.3609*10^{3}$	$1.0014*10^{2}$	$3.5054*10^{-7}$	$8.6341*10^{-2}$	$2.0021*10^{-4}$
	20	1500	47.0985	$11.0147*10^{6}$	$20.8740*10^{4}$	8.096	$4.7235*10^{3}$	$8.8986*10^{2}$	$10.4801*10^{-6}$	$9.9862*10^{-1}$	$1.3865*10^{-2}$
	30	2000	123.8977	$10.9907*10^{6}$	$33.7964*10^{5}$	17.8521	$4.1387*10^{4}$	$8.2874*10^{3}$	$19.2476*10^{-5}$	7.0062	$5.9093*10^{-1}$
f4	10	1000	-0.3492	0.3492	-0.1974	-0.0843	0.3217	-0.0536	$-8.0975*10^{-3}$	0.0239	-0.0054
	20	1500	-0.6083	0.6987	-0.2832	-0.1475	0.5689	-0.1335	$-5.1572*10^{-2}$	0.1098	-0.0762
	30	2000	-0.9074	0.9778	-0.5369	-0.2874	1.0472	-0.2273	$-6.5420*10^{-1}$	1.0732	-0.6739
f5	10	1000	-200.70	20.050	-35.900	-48.950	∞	-39.920	-45.770	∞	-16.950
f6	10	1000	20.1025	43.320	33.400	0.5641	7.2023	0.6764	$10.2476*10^{-6}$	1.0091	0.2675
	20	1500	43.6251	113.90	63.604	0.9850	13.5901	2.7048	$-13.097*10^{-5}$	2.0375	1.9952
	30	2000	56.8953	342.98	76.970	1.2674	22.9943	4.0404	$-7.1572*10^{-3}$	4.7712	2.1460
f7	10	1000	2.57632	17.9601	9.0527	0.0235	14.9423	5.0784	0	8.9951	0.4861
	20	1500	24.6741	53.4175	37.6529	0.1340	34.9604	7.9543	0	12.2865	0.6496
	30	2000	75.8731	134.7351	89.7640	0.1967	46.5347	10.9419	0	23.3989	0.8833
f8	10	1000	4.6751	22.9823	7.8431	0.2867	4.5877	0.8919	$18.6851*10^{-7}$	4.5861	0.911
	20	1500	14.8790	65.9831	19.5641	0.7462	9.6819	3.6801	$23.5638*10^{-5}$	9.6532	1.7586
	30	2000	34.5419	102.5673	47.8427	0.8793	14.8461	2.8334	$27.8790*10^{-3}$	11.7556	2.6704
f9	10	1000	3.4321	16.9652	5.8781	0.0089	36.9652	9.9947	0	26.9681	7.0441
	20	1500	6.9237	34.9879	8.0981	0.0342	78.03	8.527	0	65.0394	7.3952
	30	2000	8.4971	44.9578	10.5398	0.4531	119.11	9.579	0	119.1121	11.39
f10	10	1000	-11.8305	19.9802	-8.9839	-2.9801	0.2925	-0.618	-1	0.3192	-0.622
	20	1500	-25.7459	34.9849	-12.8568	-4.3376	0.567	-0.909	-1	0.8291	-0.761
	30	2000	-45.7969	78.0967	-22.7681	-5.9391	0.825	-0.915	-1	0.9810	-0.827

6.2. Simulation Results of MSS with Controllers

The simulation results of MSS with the three mentioned controllers will be illustrated in the following figures by using Bat and Improved-Bat Algorithms. Each figure demonstrated the Step response, bode plot and the root locus with population size of 25 bats and maximum number of generations are 100.

6.2.1. Results of different controllers based on SBA

The performance of the MS system with PD, PDF and PDFF controllers based on standard Bat algorithm has illustrated in Figures 6-8, respectively. Furthermore, the time specifications, frequency specifications and the optimal value of objective function are shown in Table 5. From the data illustrated in Table 5, clearly the time specifications (settling time, maximum peak and steady-state error) of the MS system controlled by PDFF with SBA gives better results as compared with the other techniques that utilized in this research work, and this feature appeared precisely from the minimum fitness value measure. Unfortunately, the considered system is unstable due to the negative phase margin, and that is true for all the controlling schemes.

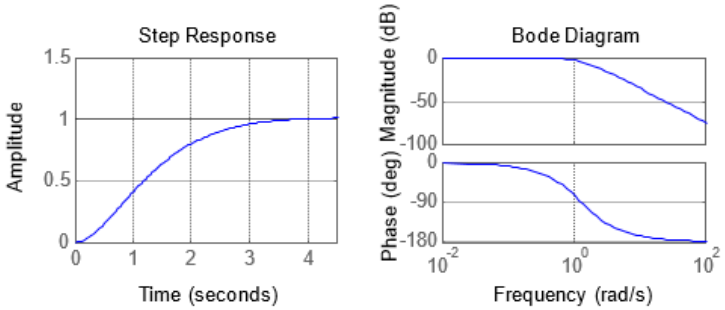

Figure 6. MSS with PD controller based on standard bat algorithm

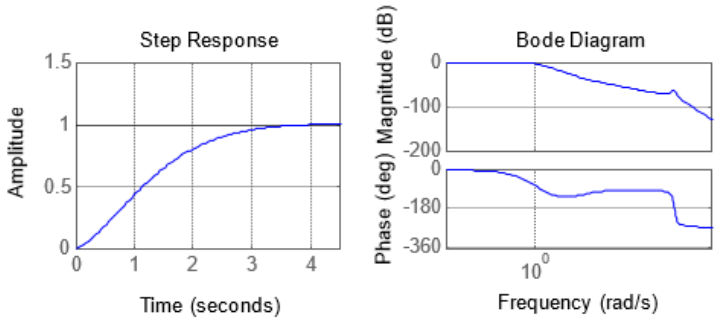

Figure 7. MSS with PDF controller based on standard bat algorithm

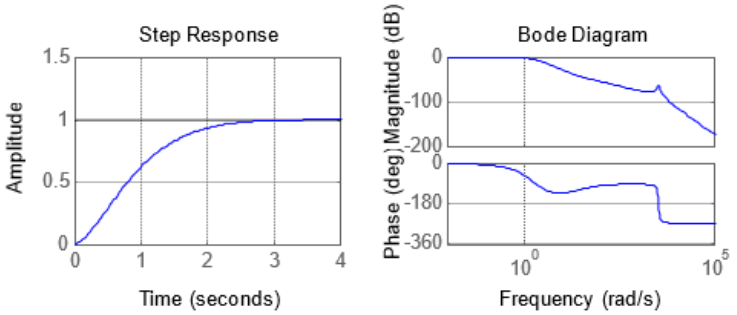

Figure 8. MSS with PDFF controller based on standard bat algorithm

Table 5. System response using standard bat algorithm

Case study	tr	ts	P.O	Ess	Gain Margin (dB)	Phase Margin (deg.)	Fitness Min
System alone	Nan	Nan	Nan	1.6702	0	3.4	-
System with PD Controller	2.1655	3.3257	0.5342	0	64.4	-180	1.9946
System with the PDF Controller	2.1441	3.3257	0.2139	0	70.4	-180	1.9255
System with the PDFF Controller	1.9235	2.2613	0.1021	0	78.6	-180	1.6721

6.2.2. Results of different controllers based on IBA

The performance of the MS system with PD, PDF and PDFF controllers based on proposed improved Bat algorithm has depicted in Figures 9-11, respectively. Furthermore, the time and frequency specifications as well as the optimal value of objective function are summarized in Table 6. From the results showed in Table 6, it is worthy to mention that the time parameters as well as frequency parameters of the MS system controlled by PDFF with proposed IBA can be considered the dominant structure that gives the faster and accurate response with a good margin of magnitude and phase. Therefore, the suggested modifications on SBA can be considered as an effective improvement after applied on the selected complex benchmark functions and on the maglev system

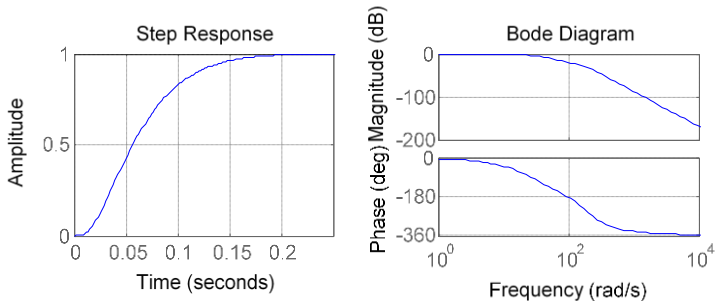

Figure 9. MSS with PD controller based on improved bat algorithm

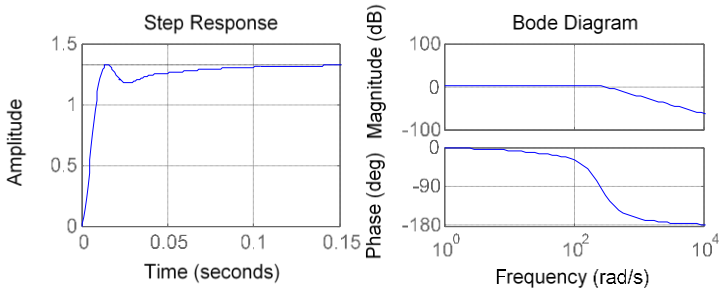

Figure 10. MSS with PDF controller based on improved bat algorithm

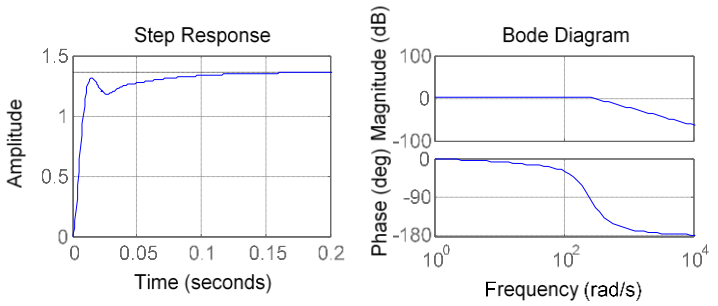

Figure 11. MSS with PDFF controller based on improved bat algorithm

Table 6. System response using improved bat algorithm

Case study	tr	ts	P.O	Ess	Gain Margin (dB)	Phase Margin (deg.)	Fitness Min
System with PD Controller	0.0535	0.1831	0	0.2606	23.45	-180	0.1391
System with the PDF Controller	0.0092	0.1018	0	0.1920	∞	80.27	0.0986
System with the PDFF Controller	0.0065	0.0896	0	0.0965	∞	87.98	0.0645

7. CONCLUSION

The mathematical modeling and controlling of magnetic suspending system had been investigated in this research paper. The controller design includes: PD control, PDF control and PDFF control. The proposed controlling schemes are implemented and verified in Matlab environment for magnetic suspending system stabilization. The controllers' parameters are tuned by optimizing the fitness function using SBA and proposed IBA method. A new algorithm based on Bat algorithm has been proposed to solve complex optimization problems. To demonstrate the effectiveness, reliability and robustness of the proposed algorithm, a set of well selected benchmark optimization problems. The results of comparison showed that IBA gives significant results in lesser time and with fewer numbers of iterations and enhances the local and global search capability of the SBA and PSO algorithms. Therefore, it is feasible to select IBA to tune the considered controllers for the maglev system. The simulation results of MS system with different controlling techniques have shown that PDFF based on proposed IBA scheme had outperformed on BA in terms of time and frequency specifications as well as in enhancing the maglev system stability.

REFERENCES

[1] S. Yadav, *et al*., "Optimized PID Controller for Magnetic Levitation System," *IFAC-Papers OnLine*, vol. 49, no. 1, pp. 778-782, 2016.

[2] S. Yadav, *et al*., "Performance Enhancement of Magnetic Levitation System using Teaching Learning based Optimization," *Alexandria Engineering Journal*, vol. 57, no. 4, pp. 2427-2433, 2018.

[3] R. Song and Z. Chen, "Design of PID Controller for Maglev System Based on an Improved PSO with Mixed Inertia Weight," *Journal of Networks*, vol. 9, no. 6, pp. 1509-1517, Jun. 2014.

[4] I. Ahmad, *et al*., "Optimal PID Control of Magnetic Levitation System Using Genetic Algorithm," In *Proceedings of IEEE International Energy Conference (ENERGYCON)*, Cavtat, Croatia, pp. 1429-1433, May 2014.

[5] S. A. Al-Samarraie, "Variable Structure Control Design for a Magnetic Levitation System," *Journal of Engineering*, vol. 24, no. 12, pp. 84-103, Dec. 2018.

[6] A.- V. Duka, *et al*., "IMC based PID Control of a Magnetic Levitation System," *Procedia Technology*, vol. 22, pp. 592-599, 2016.

[7] N. Mukherjee, "System Identification and State Feedback Controller Design of Magnetic Levitation System," *International Journal of Engineering and Technical Research*, vol. 2, no. 6, pp. 158-163, Jun. 2014.

[8] A. A. Awelewa, *et al*., "An Undergraduate Control Tutorial on Root Locus-Based Magnetic Levitation System Stabilization," *International Journal of Engineering Computer Science*, vol. 13, no. 13, pp. 14-22, 2013.

[9] D. S. Shu'aibu, *et al*., "Efficient Fuzzy Logic Controller for Magnetic Levitation Systems," *Nigerian Journal of Technological Development*, vol. 13, no. 2, pp. 50-57, 2016.

[10] M. Golob and B. Tovornik, "Modeling and Control of the Magnetic Suspension System," *ISA Transactions*, vol. 42, no. 1, pp. 89-100, 2003.

[11] A. H. Fares, *et al*., "Intelligent Control of Magnetic Levitation System," *Journal of Engineering Sciences*, Assiut University, vol. 37, no. 4, pp. 909-924, Jul. 2009.

[12] W. Chen, *et al*., "PID Controller Design of Maglev Ball System based on Chaos Parameters Optimization," In *Proceedings of International Conference on Machine Vision and Human-Machine Interface*, Kaifeng, China, pp. 772-775, Apr. 2010.

[13] N. F. Al-Muthairi and M. Zribi, "Sliding Mode Control of a Magnetic Levitation System," *Mathematical Problems in Engineering*, vol. 2004, no. 2, pp. 93-107, 2004.

[14] W. Bariet and J. Chiasson, "Linear and Nonlinear State-space Controllers for Magnetic Levitation," *International Journal of Systems Science*, vol. 27, no. 11, pp. 1153-1163, 1996.

[15] D. L. Trumper, S. M. Olson and P. K. Subrahmanyan, "Linearizing control of magnetic suspension systems," in *IEEE Transactions on Control Systems Technology*, vol. 5, no. 4, pp. 427-438, Jul. 1997.

[16] I. Ž. Nikolić and I. Milivojević, "Application of Pseudo-Derivative Feedback in Industrial Robots Controllers," *The Scientific Journal FACTA UNIVERSITATIS, Mechanics, Automatic Control and Robotics*, vol. 2, no. 8, pp. 741-756, 1998.

[17] G. A. Hassaan, "Tuning of a PDFF Controller used with a Very Slow Second Order Process," *International Journal of Advanced Research in Computer Science & Technology*, vol. 2, no. 3, pp. 175-178, 2014.

[18] X.-S. Yang, "A New Metaheuristic Bat-Inspired Algorithm," In *Nature Inspired Cooperative Strategies for Optimization (NICSO 2010)*, (Eds. J.R. González *et al*.), *Studies in Computational Intelligence*, Springer, Berlin, Germany, pp.65-74, 2010.

[19] B. V. Rao and G. V. N. Kumar, "Optimal Power Flow by Bat Search Algorithm for Generation Reallocation with Unified Power Flow Controller," *International Journal of Electrical Power and Energy Systems*, vol. 68, no. 3, pp. 81-88, Jun. 2015.

[20] K. Premkumar and B. V. Manikandan, "Bat Algorithm Optimized Fuzzy PD baesd Speed Controller for Brushless Direct Current Motor," *Engineering Science and Technology, an International Journal*, vol. 19, no. 2, pp. 818-840, Jun. 2016.

[21] S. Srivastava and S. K. Sahana, "Application of Bat Algorithm for Transport Network Design Problem," *Applied Computational Intelligence and Soft Computing*, vol. 2019, pp. 1-12, 2019.

[22] M. R. Ramli, *et al*., "Enhanced Convergence of Bat Algorithm based on Dimensional and Inertia Weight Factor," *Journal of King Saud University-Computer and Information Sciences*, 2018.

[23] N. H. Abbas, and R. A. Humadi, "Load Flow Computation of Power System with SVC using Improved PSO Algorithms," In *Proceedings of Fifth International Joint Conferences on CNC 2014 and CCPE 2014*, Chennai, India, Feb. 2014.

[24] A. Kaveh and P. Zakian, "Enhanced Bat Algorithm for optimal Design of Skeletal Structures," *Asian Journal of Civil Engineering*, vol. 15, no. 2, pp. 179-212, 2014.

[25] X.-S. Yang, "Nature-Inspired Optimization Algorithms," *Elsevier Insights, 1st Edition*, 2014.

BIOGRAPHY OF AUTHOR

Nizar Hadi Abbas was born in Baghdad, 1975. He received his B.Sc. degree in electrical engineering from University of Baghdad, Baghdad, Iraq in 2000, an M.Sc. degree in control and computer engineering in 2002 from University of Baghdad, and a Ph.D. degree in advanced control in 2011 from Osmania University, Hyderabad, India. He is presently an assistant professor. His research interests include control theory, controllers design, fractional order systems, robot modeling & control and modern optimization techniques. He published 20 scientific articles and coauthored one book.